

Cross-Correlating Cosmic Microwave Background Radiation Fluctuations with Redshift Surveys: Detecting the Signature of Gravitational Lensing

Maki Suginoara^{1,2}, Tatsushi Suginoara^{1,3,4}, and David N. Spergel^{5,6}

Department of Astrophysical Sciences, Princeton University, Princeton, NJ 08544

ABSTRACT

Density inhomogeneities along the line-of-sight distort fluctuations in the cosmic microwave background. Usually, this effect is thought of as a small second-order effect that mildly alters the statistics of the microwave background fluctuations. We show that there is a first-order effect that is potentially observable if we combine microwave background maps with large redshift surveys. We introduce a new quantity that measures this lensing effect, $\langle T(\delta\boldsymbol{\theta} \cdot \nabla T) \rangle$, where T is the microwave background temperature and $\delta\boldsymbol{\theta}$ is the lensing due to matter in the region probed by the redshift survey. We show that the expected signal is first order in the gravitational lensing bending angle, $\langle (\delta\boldsymbol{\theta})^2 \rangle^{1/2}$, and find that it should be easily detectable, $(S/N) \sim 15 - 35$, if we combine the Microwave Anisotropy Probe satellite and Sloan Digital Sky Survey data. Measurements of this cross-correlation will directly probe the “bias” factor, the relationship between fluctuations in mass and fluctuations in galaxy counts.

Subject headings: cosmology: cosmic microwave background, gravitational lensing

¹Department of Physics, the University of Tokyo, Tokyo 113, Japan

²makis@astro.Princeton.EDU, JSPS Research Fellow

³RESCEU, School of Sciences, the University of Tokyo, Tokyo 113, Japan

⁴tatsushi@astro.Princeton.EDU, JSPS Postdoctoral Fellow

⁵Department of Astronomy, University of Maryland, College Park, MD 20742

⁶dns@astro.Princeton.EDU

1. Introduction

The next several years should be very exciting for cosmologists: Microwave Anisotropy Probe (MAP; Wright et al. 1996) and PLANCK (Bouchet et al. 1995) will make high resolution maps of the microwave background sky; while the Sloan Digital Sky Survey (SDSS; Gunn and Weinberg 1995; see also <http://www-sdss.fnal.gov:8000/>) will measure redshifts of 10^6 galaxies and positions of 10^8 galaxies. In this paper, we explore the *direct* connection between these two measurements through gravitational lensing: the path of a cosmic microwave background (CMB) photon is distorted by inhomogeneities in the matter distribution; galaxy surveys detect these inhomogeneities as fluctuations in galaxy number counts.

The effect of the gravitational lensing on the CMB anisotropies has been studied by many authors. The uncomfortably low upper limits (Uson and Wilkinson 1984, Readhead et al. 1989) provoked a great deal of controversy (Kashlinsky 1988, Tomita 1988, Sasaki 1989, Watanabe and Tomita 1991) about the possibility that gravitational lensing washes out the intrinsic fluctuation. After the detection by the Cosmic Background Explorer (COBE; Smoot et al. 1992), there has been renewal of interest (Linder 1990a, b, Cayón et al. 1993a, b, Seljak 1996) in investigating how the CMB power spectrum is redistributed owing to gravitational lensing. For example, Seljak (1996) recently presented detailed calculations of gravitationally deflected CMB power spectra, including the effect of the nonlinear evolution of matter density fluctuations. His result shows, however, that the modification of the CMB power spectrum is a second-order effect of the photon bending angle and less than a few percent on angular scales greater than ten arcminutes. Hence, the lensing effect on the CMB spectrum itself is extremely difficult to detect, even with observations such as the MAP project. Linder (1997) has also studied the effects of lensing on the correlation function and has introduced a cross-correlation function similar to the one that we study here.

In this paper, we introduce a cross-correlation function that is sensitive to the gravitational lensing correlations between the temperature fluctuations and matter density fluctuations. We show that the cross-correlation is first-order in the bending angle so it should be easier to detect if we have both accurate CMB maps and redshift surveys. We quantitatively estimate its magnitude and its cosmic variance in cold dark matter (CDM) universes. The rest of the paper is organized as follows. We review the formalism developed by Seljak (1996) for computing the angular excursion of the CMB photon paths on celestial sphere in section 2. In section 3, we formulate the cross-correlation between matter density inhomogeneities and CMB temperature fluctuations. Section 4 concludes.

2. Gravitational Lensing

In this section, we review gravitational lensing by density fluctuations. We follow the power spectrum approach of Seljak (1994, 1996). We focus on the angular excursions produced by matter

fluctuations at low redshifts, where they can be most easily inferred from redshift surveys.

Fluctuations in matter density, δ , generate variations in the gravitational potential,

$$\nabla^2 \phi = 4\pi G \rho_b a^2 \delta, \quad (1)$$

where G is the gravitational constant, and ρ_b is the mean background mass density. Conventionally, the matter density fluctuations are related to the fluctuations in galaxy counts by a linear biasing parameter, b :

$$\delta_g = b \delta. \quad (2)$$

Since most of the lensing effects will be produced by fluctuations on large physical scales ($k < 0.1h^{-1}\text{Mpc}$), the linear biasing model will hopefully be valid. It is important to note that detailed nonlinear and/or time-dependent biasing may somewhat change the statistics we present in this paper.

A photon emitted at some angular position $\boldsymbol{\theta}$ has been deflected by gravitational lensing during its long travel, with the result that it is observed at different angular position, $\boldsymbol{\psi}$. The photon angular excursion on celestial sphere is given by Seljak (1994):

$$\boldsymbol{\theta} - \boldsymbol{\psi} = \delta\boldsymbol{\theta}(z) = -2 \int_0^{\chi(z)} d\chi' W(\chi', \chi_{\text{dec}}) \nabla_{\perp} \phi, \quad (3)$$

where ∇_{\perp} is transverse component of the potential gradient with respect to the photon path,

$$W(\chi, \chi_{\text{dec}}) = \sin_K(\chi_{\text{dec}} - \chi) / \sin_K(\chi_{\text{dec}}) \quad (4)$$

is a projection operator on celestial sphere, and $\chi_{\text{dec}} = \chi(z_{\text{dec}})$ is unperturbed comoving radial distance corresponding to redshift z_{dec} at decoupling time. In equation (4), $\sin_K(u) = \sin(u)$, u , and $\sinh(u)$ in a closed, flat, and open universe, respectively.

Next, we consider the relative angular excursion $\delta\boldsymbol{\theta} - \delta\boldsymbol{\theta}'$ of a photon pair emitted from angular positions $\boldsymbol{\theta}$ and $\boldsymbol{\theta}'$. We restrict our calculation to the small angular separation limit, $\xi = |\boldsymbol{\theta} - \boldsymbol{\theta}'| \ll 1$, and assume that the relative angular excursion $\delta\boldsymbol{\theta} - \delta\boldsymbol{\theta}'$ obeys Gaussian statistics. Lensing is primarily due to scattering events from mass fluctuations on the 10 - 100 Mpc scale. As there are 30 - 300 of these fluctuations between the surface of last scatter and the present along each photon path, the central limit theorem implies that this is a good approximation. Following Seljak (1994), we characterize the statistics of the lensing fluctuations by its root-mean-square dispersion:

$$\begin{aligned} \sigma(\xi; z) &= 2^{-1/2} \left\langle [\delta\boldsymbol{\theta}(z) - \delta\boldsymbol{\theta}'(z)]^2 \right\rangle_{\xi}^{1/2} = [C_{\text{gl}}(0; z) - C_{\text{gl}}(\xi; z)]^{1/2}, \\ C_{\text{gl}}(\xi; z) &\equiv \frac{2}{\pi} \int_0^{\infty} k^3 dk \int_0^{\chi(z)} d\chi' P_{\phi}(k, \tau_0 - \chi') W^2(\chi', \chi_{\text{dec}}) J_0(k\xi \sin_K \chi'), \end{aligned} \quad (5)$$

where $\langle \rangle_{\xi}$ denotes the averaging over pairs observed with fixed angular separation ξ , J_0 is the Bessel function of order 0, and $P_{\phi}(k)$ is the gravitational potential power spectrum. The power

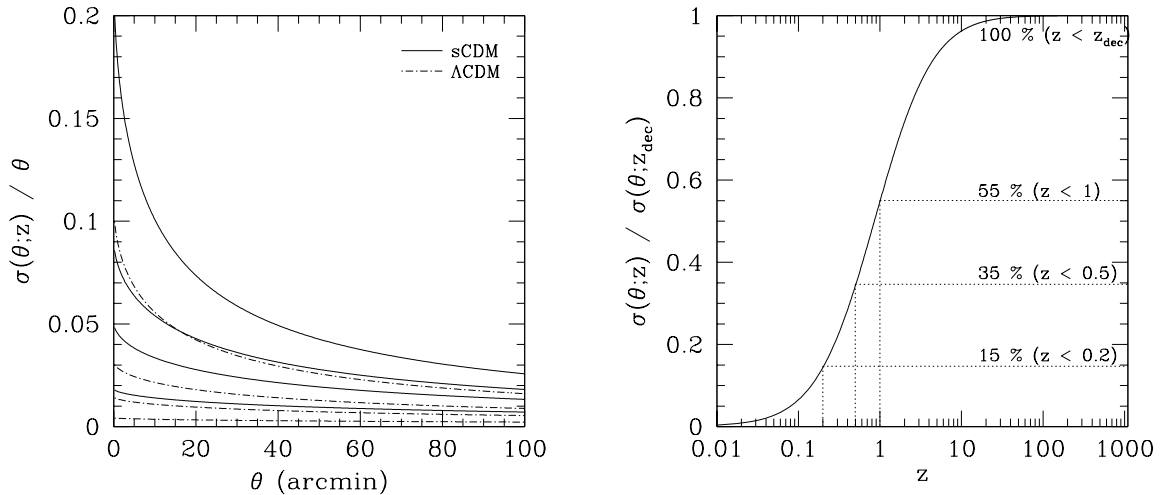


Fig. 1.— The dispersion of the relative angular excursion, $\sigma(\theta; z)$. 1a: Dependence on the separation angle θ . Solid lines show the standard cold dark matter (SCDM) model with $\Omega_{m0} = 1$, $\Omega_{v0} = 0$, $h = 0.5$, and $\sigma_8 = 1.2$. Broken lines show the cosmological constant dominated cold dark matter (Λ CDM) model with $\Omega_{m0} = 0.3$, $\Omega_{v0} = 0.7$, $h = 0.7$, and $\sigma_8 = 1.0$. For each model, the curves show the case in which $z = z_{\text{dec}}$, 1, 0.5, and 0.2, from upper to lower. 1b: Dependence on the redshift z at $\theta = 0.21$ degree in the SCDM model.

spectrum of the potential fluctuations are related to the power spectrum of the density fluctuations through,

$$P_\phi(k, \tau) = (9/4)\Omega_m^2(\tau)H^4(\tau)a^4(\tau)k^{-4}P(k, \tau), \quad (6)$$

where Ω_m is the mass density parameter given by $\Omega_m \equiv 8\pi G\rho_b/(3H^2)$, and $H(\tau)$ is the Hubble parameter.

Figure 1a shows $\sigma(\theta; z)$ as functions of θ for several redshift values. We consider throughout this paper two cosmological models: one is the standard CDM (SCDM) model with $\Omega_{m0} = 1$, $\Omega_{v0} = 0$, $h = 0.5$, and $\sigma_8 = 1.2$, and the other is a low-density, cosmological constant dominated CDM (Λ CDM) model with $\Omega_{m0} = 0.3$, $\Omega_{v0} = 0.7$, $h = 0.7$, and $\sigma_8 = 1.0$, the best fit model of Ostriker and Steinhardt (1995). Here, Ω_{m0} and Ω_{v0} are the present mass density and the present vacuum energy density normalized by the critical density; h is the present Hubble parameter in units of $100 \text{ km s}^{-1} \text{ Mpc}^{-1}$; σ_8 is the mass fluctuations within a sphere of radius $8 h^{-1} \text{ Mpc}$. We use the COBE normalized value (Bunn and White 1997) for σ_8 . In numerical calculation of $\sigma(\xi; z)$, we have used the fitting formula for CDM linear transfer function given in Bardeen et al. (1986).

The SDSS project measures the redshift of galaxies up to $z \simeq 0.2$ within solid angle $\Omega_{\text{SDSS}} = \pi$ steradian. Furthermore, we expect to obtain photometric redshifts (Connolly et al. 1995) of galaxies up to $z \simeq 1$ with fairly small uncertainties. Then we will obtain the galaxy

number density perturbation, $\delta_g(\mathbf{r})$, within solid angle Ω_{SDSS} for $z < 0.2$, and for $z < 1$ with some uncertainties due to error in photometric redshifts. We can see from Figures 1b that the matter within $z < 0.2$, $z < 0.5$, and $z < 1$ contributes 15%, 35%, and 55%, respectively, to the angular excursion from the last scattering surface. Hereafter, the values with subscript A denote the integral from the observer to some redshift z , the edge of the survey data, and those with subscript B denote the integral over remaining part; for example:

$$\delta\boldsymbol{\theta}_A = -2 \int_0^{\chi(z)} d\chi' W(\chi', \chi_{\text{dec}}) \nabla_{\perp} \phi, \quad (7)$$

$$\delta\boldsymbol{\theta}_B = -2 \int_{\chi(z)}^{\chi_{\text{dec}}} d\chi' W(\chi', \chi_{\text{dec}}) \nabla_{\perp} \phi. \quad (8)$$

The total lensing deviation, $\delta\boldsymbol{\theta} = \delta\boldsymbol{\theta}_A + \delta\boldsymbol{\theta}_B$. Its variance is the sum of the contribution from the two regions:

$$\langle (\delta\boldsymbol{\theta})^2 \rangle = \langle (\delta\boldsymbol{\theta}_A)^2 \rangle + \langle (\delta\boldsymbol{\theta}_B)^2 \rangle \equiv 2(\sigma_A^2 + \sigma_B^2). \quad (9)$$

For our purposes, the distant lensing is unimportant; its only effect is to slightly reduce the amplitude of the temperature fluctuations.

3. Lensing the Microwave Background

Gravitational lensing distorts the microwave background sky:

$$\tilde{T}(\boldsymbol{\psi}) = T[\boldsymbol{\theta}(\boldsymbol{\psi})] = T(\boldsymbol{\psi} + \delta\boldsymbol{\theta}) = T(\boldsymbol{\psi}) + \delta\boldsymbol{\theta} \cdot \nabla T(\boldsymbol{\psi}) + \frac{1}{2} [\delta\boldsymbol{\theta} \cdot \nabla]^2 T(\boldsymbol{\psi}) + \dots \quad (10)$$

Here \tilde{T} denotes the measured temperature map and T denotes the unlensed temperature map.

This distortion alters the statistics of the microwave background by smearing out temperature correlations (Seljak 1996):

$$\begin{aligned} \langle \tilde{T}(\boldsymbol{\psi}) \tilde{T}(\boldsymbol{\psi}') \rangle &= \langle T(\boldsymbol{\psi}) T(\boldsymbol{\psi}') \rangle + \langle [\delta\boldsymbol{\theta} \cdot \nabla T(\boldsymbol{\psi})] [\delta\boldsymbol{\theta}' \cdot \nabla T(\boldsymbol{\psi}')] \rangle \\ &\quad + \langle T(\boldsymbol{\psi}) (\delta\boldsymbol{\theta}' \cdot \nabla)^2 T(\boldsymbol{\psi}') \rangle. \end{aligned} \quad (11)$$

This can be alternatively written in terms of the correlation function:

$$C_{\text{lensed}}(\xi) = C_{\text{unlensed}}(\xi) + \frac{\sigma^2}{2} \frac{\partial^2 C_{\text{unlensed}}(\xi)}{\partial \xi^2}, \quad (12)$$

where $\xi = |\boldsymbol{\psi} - \boldsymbol{\psi}'|$.

If we have a redshift survey, then the effects of gravitational lensing of the microwave background can be observed more easily. Here, we introduce a new quantity, H , which measures the cross-correlation between the temperature map and the predicted lensing:

$$H(\xi) = \mathcal{N} \langle \tilde{T}(\boldsymbol{\psi}) \left([\delta\boldsymbol{\theta}_A - \delta\boldsymbol{\theta}'_A] \cdot \nabla \tilde{T}(\boldsymbol{\psi}') \right) \rangle_{\xi}, \quad (13)$$

where $\delta\boldsymbol{\theta}_A(\boldsymbol{\psi})$ is determined from the redshift survey, and \mathcal{N} is a normalization factor given by

$$\mathcal{N}^{-1} \equiv \sigma_A(\theta_{\text{fwhm}}) \left\langle T^2 \right\rangle_{\theta_{\text{fwhm}}}^{1/2} \left\langle (\nabla T)^2 \right\rangle_{\theta_{\text{fwhm}}}^{1/2} \quad (14)$$

at a typical value of angular separation $\theta = \theta_{\text{fwhm}}$.

We can evaluate this by expanding the temperature map in a Fourier series. Since the lensing bending angles are small, we simplify the equations by making the plane parallel approximation and expanding out the unlensed temperature map:

$$T(\boldsymbol{\theta}) = \sum_{\boldsymbol{l}} a_{\boldsymbol{l}} \exp(-i\boldsymbol{l} \cdot \boldsymbol{\theta}), \quad (15)$$

where $a_{\boldsymbol{l}}$ denotes multipole moments. We can now rewrite the effects of lensing in the multipole expansion:

$$\begin{aligned} \tilde{T}(\boldsymbol{\psi}) &= T(\boldsymbol{\psi} + \delta\boldsymbol{\theta}) \\ &= \sum_{\boldsymbol{l}} a_{\boldsymbol{l}} \exp[-i\boldsymbol{l} \cdot (\boldsymbol{\psi} + \delta\boldsymbol{\theta})], \end{aligned} \quad (16)$$

and

$$\frac{\partial \tilde{T}(\boldsymbol{\psi}')}{\partial \boldsymbol{\psi}'} = \sum_{\boldsymbol{l}'} i\boldsymbol{l}' a_{\boldsymbol{l}'}^* \exp[i\boldsymbol{l}' \cdot (\boldsymbol{\psi}' + \delta\boldsymbol{\theta}')]. \quad (17)$$

We can now evaluate the lensing statistic:

$$\begin{aligned} H(\xi) &= \mathcal{N} \sum_{\boldsymbol{l}} \sum_{\boldsymbol{l}'} \left\langle a_{\boldsymbol{l}} a_{\boldsymbol{l}'}^* \exp(-i\boldsymbol{l} \cdot \delta\boldsymbol{\theta} + i\boldsymbol{l}' \cdot \delta\boldsymbol{\theta}') \right. \\ &\quad \left. \times [i\boldsymbol{l} \cdot (\delta\boldsymbol{\theta}_A - \delta\boldsymbol{\theta}'_A)] \exp(-i\boldsymbol{l} \cdot \boldsymbol{\psi} + i\boldsymbol{l}' \cdot \boldsymbol{\psi}') \right\rangle \\ &= \mathcal{N} \sum_{\boldsymbol{l}} \left\langle a_{\boldsymbol{l}}^2 \right\rangle \exp[-i\boldsymbol{l} \cdot (\boldsymbol{\psi} - \boldsymbol{\psi}')] \\ &\quad \times \langle i\boldsymbol{l} \cdot (\delta\boldsymbol{\theta}_A - \delta\boldsymbol{\theta}'_A) \exp[-i\boldsymbol{l} \cdot (\delta\boldsymbol{\theta}_A - \delta\boldsymbol{\theta}'_A)] \rangle \\ &\quad \times \langle \exp[-i\boldsymbol{l} \cdot (\delta\boldsymbol{\theta}_B - \delta\boldsymbol{\theta}'_B)] \rangle. \end{aligned} \quad (18)$$

Since the gravitational deflections are the sum of many small scattering due to superclusters and voids along the line-of-sight, we can treat $x = \boldsymbol{l} \cdot (\delta\boldsymbol{\theta} - \delta\boldsymbol{\theta}')$ as a Gaussian random variable. The dispersion of x is $\langle x^2 \rangle = l^2 \sigma^2$, where we have kept only the main isotropic term. The anisotropic term makes a subdominant contribution to the gravitational lensing effect on two-point auto-correlation function of CMB (Seljak 1996, Martínez-González et al. 1997). Though the anisotropic term is not too small in this statistics, the more rigorous analysis will be given in a subsequent paper (Suginohara, Suginohara and Spergel 1997). Then

$$\langle ix \exp(-ix) \rangle = - \sum_{n=0}^{\infty} \frac{\langle (-ix)^{n+1} \rangle}{n!} \quad (19)$$

$$\begin{aligned}
&= \sum_{n=0}^{\infty} \frac{(-1)^n}{(2n+1)!} (2n+1)!! \langle x^2 \rangle^{n+1} \\
&= l^2 \sigma^2 \exp\left(-\frac{l^2 \sigma^2}{2}\right).
\end{aligned}$$

Combining equations (18) and (19),

$$\begin{aligned}
H(\xi) &= \mathcal{N} \sum_{\mathbf{l}} \langle a_{\mathbf{l}}^2 \rangle l^2 \sigma_A^2(\xi) \exp\left[-\frac{l^2 \sigma_A^2(\xi)}{2}\right] \exp[-i\mathbf{l} \cdot (\boldsymbol{\psi} - \boldsymbol{\psi}')] \\
&\quad \times \exp\left[-\frac{l^2 \sigma_B^2(\xi)}{2}\right].
\end{aligned} \tag{20}$$

The final term represents the smearing of the microwave fluctuations due to density fluctuations beyond the edge of the redshift survey. This effect is a small correction term, which we will ignore for the remainder of the paper.

We average equation (20) over angle and rewrite it on the celestial sphere, then

$$H(\xi) = \mathcal{N} \sum_{\mathbf{l}} C_l W_l \frac{(2l+1)}{4\pi} l^2 \sigma_A^2(\xi) \exp\left[-\frac{l^2 \sigma_A^2(\xi)}{2}\right] P_l(\cos \xi), \tag{21}$$

where ξ is the angular separation on the sky, C_l is the usual multipole moment, $W_l = \exp(-l^2 \sigma_{\text{beam}}^2)$ is the window function, and σ_{beam} is the beam of the detector (Knox 1995).

The cosmic variance in the cross-correlation statistic can also be estimated by taking the leading order term in the expansion:

$$\begin{aligned}
\langle H^2 \rangle &= \mathcal{N}^2 \left\langle \left[\tilde{T}(\boldsymbol{\psi}) \left([\delta\boldsymbol{\theta} - \delta\boldsymbol{\theta}'] \cdot \nabla \tilde{T}(\boldsymbol{\psi}') \right) \right]^2 \right\rangle \\
&\simeq \mathcal{N}^2 \sigma_A^2(\xi) \langle T^2 \rangle \langle (\nabla T)^2 \rangle.
\end{aligned} \tag{22}$$

Note that the signal-to-cosmic variance scales as $\langle H \rangle / \langle H^2 \rangle^{1/2}$, which is proportional to σ_A . As we claimed earlier, this is a first-order effect.

We can estimate the signal-to-cosmic variance ratio by computing the predicted signal per multipole:

$$\begin{aligned}
H_{\mathbf{l}} &= \int d\boldsymbol{\psi} d\boldsymbol{\psi}' \tilde{T}_{\mathbf{l}}(\boldsymbol{\psi}) (\delta\boldsymbol{\theta}(\boldsymbol{\psi}) - \delta\boldsymbol{\theta}'(\boldsymbol{\psi}')) \cdot \nabla \tilde{T}_{\mathbf{l}}^*(\boldsymbol{\psi}') \\
&= \int d\boldsymbol{\psi} d\boldsymbol{\psi}' a_{\mathbf{l}} \exp[-i\mathbf{l} \cdot (\boldsymbol{\psi} + \delta\boldsymbol{\theta})] [i\mathbf{l} \cdot (\delta\boldsymbol{\theta}(\boldsymbol{\psi}) - \delta\boldsymbol{\theta}'(\boldsymbol{\psi}'))] \\
&\quad \times a_{\mathbf{l}}^* \exp[i\mathbf{l} \cdot (\boldsymbol{\psi}' + \delta\boldsymbol{\theta}')] \\
&\simeq C_l W_l l^2 \sigma_l^2 \exp(-l^2 \sigma_l^2 / 2),
\end{aligned} \tag{23}$$

where $\sigma_l = \sigma_A(\pi/l)$. If we include detector noise, then

$$\begin{aligned}\langle T_l^2 \rangle &= C_l W_l + w^{-1}, \\ \langle (\nabla T)_l^2 \rangle &= l^2 (C_l W_l + w^{-1}),\end{aligned}\tag{24}$$

where w^{-1} is the measure of the detector noise (Knox 1995). MAP’s highest frequency channel has a full width at half maximum of 0.21 degree and a system noise of $w^{-1} = (10.5\mu\text{K})^2 \text{ degree}^2 = (0.18\mu\text{K})^2 \text{ steradian}$. By combining the three highest frequency channel, the MAP system noise drop to $(0.11\mu\text{K})^2 \text{ steradian}$. This implies that the noise plus cosmic variance in H_l is

$$\langle (H_l)^2 \rangle = \frac{l^2 \sigma_l^2}{2l+1} (C_l W_l + w^{-1})^2,\tag{25}$$

where the factor of $2l+1$ comes from averaging over all multipoles with the same l . Note that there is no factor of 2 in the numerator as the variance is proportional to the product of two uncorrelated fields, $\langle T^2 (\nabla T)^2 \rangle$, rather than the more familiar $\langle T^4 \rangle - \langle T^2 \rangle^2 = 2 \langle T^2 \rangle^2$. Summing over all multipoles yields the expected signal in the microwave maps:

$$\begin{aligned}\left(\frac{S}{N}\right)^2 &= \sum_l \frac{\langle H_l \rangle^2}{\langle (H_l)^2 \rangle} \\ &= \sum_l (2l+1) \frac{l^2 \sigma_l^2 \exp(-l^2 \sigma_l^2)}{[1 + (w C_l W_l)^{-1}]^2}.\end{aligned}\tag{26}$$

Note that an additional cross-correlation function that can be computed from the microwave background fluctuations and the lensing maps:

$$G(\xi) = \left\langle \tilde{T}(\boldsymbol{\psi}) \left([\delta\boldsymbol{\theta}_A(\boldsymbol{\psi}) - \delta\boldsymbol{\theta}'_A(\boldsymbol{\psi}')] \cdot \hat{\mathbf{n}} \tilde{T}(\boldsymbol{\psi}') \right) \right\rangle_{\xi},\tag{27}$$

where $\hat{\mathbf{n}} = \frac{(\boldsymbol{\psi} - \boldsymbol{\psi}')}{|\boldsymbol{\psi} - \boldsymbol{\psi}'|}$. The statistics has the simplest form among possible inclusions of gravitational lensing angular excursion. The cross-correlation function is reduced to

$$G(\xi) = \mathcal{N}_G \sigma_A^2 \frac{\partial C(\xi)}{\partial \xi}.\tag{28}$$

However we confirmed that the expected signal-to-noise ratio, S/N , in G is lower than in H . This is because, unlike in H , the cosmic variance in G contains a term proportional to $\langle T^2(\boldsymbol{\psi}) T^2(\boldsymbol{\psi}') \rangle$.

4. Results and Discussion

We have computed the expected cross-correlation between the temperature fluctuations and the lensing bending angle (equation (21)) for the standard CDM model and the “best fit” vacuum

dominated model (Ostriker and Steinhardt 1995). In estimating the lensing bending angle, we have assumed that we have a redshift survey that extends to a characteristic redshift z . Figure 2 shows the results for large scale surveys of varying depths. In this figure, we have assumed the standard parameters for the MAP and SDSS projects. The characteristic depth of the SDSS redshift survey is $z = 0.2$. SDSS has photometric redshifts for 10^8 galaxies that should extend the survey to $z = 1$. These photometric redshifts are accurate to ± 0.02 in redshift; certainly accurate enough to compute the projected surface densities needed to predict lensing. Figure 3 shows the cumulative signal-to-noise, where we have summed over all of the multipoles. We have divided (S/N) in equation (26) by a factor of 2 taking into account the limited sky coverage, Ω_{SDSS} . The predicted signal-to-noise is quite large (15 and 35) for the vacuum-dominated and standard CDM models.

This cross-correlation, if detected, directly probes the gravitational potential fluctuations at low redshift. In principle, it should yield an accurate determination of the biasing factor. Armed with this measurement, we should be able to directly compare the gravitational potential fluctuations at decoupling with the gravitational potential fluctuations in the local universe.

We thank Seljak and Zaldarriaga for providing their code to generate the intrinsic CMB power spectrum. DNS acknowledges the MAP/MIDEX project for support. MS and TS acknowledge support from Research Fellowships of the Japan Society for the Promotion of Science.

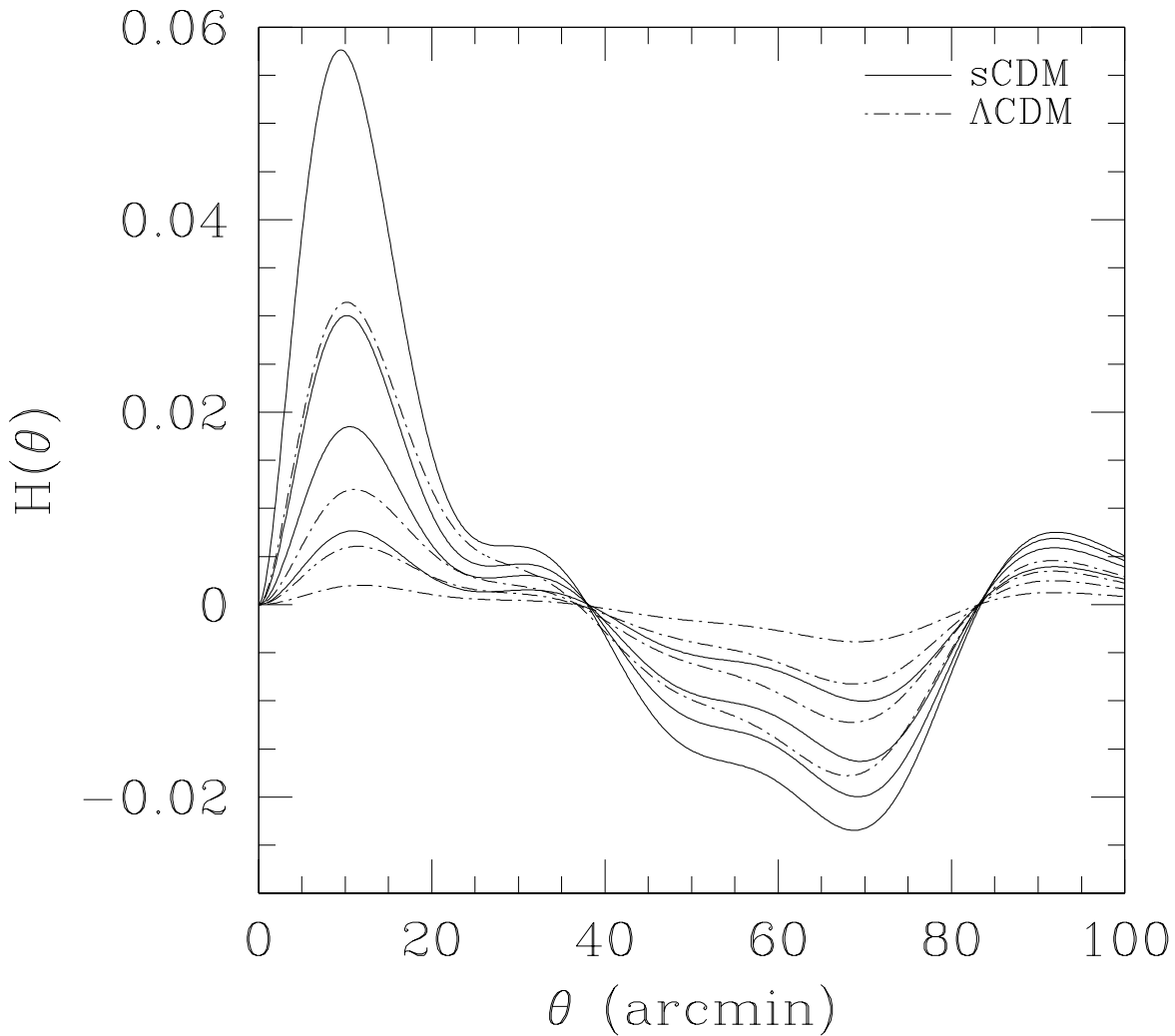


Fig. 2.— The cross-correlation, $H(\theta)$, for $\theta_{\text{fwhm}} = 0.21$ degree. Solid and broken lines show the SCDM model and the Λ CDM model as in Fig. 1. For each model, the curves show the case in which $z = z_{\text{dec}}$, 1, 0.5, and 0.2.

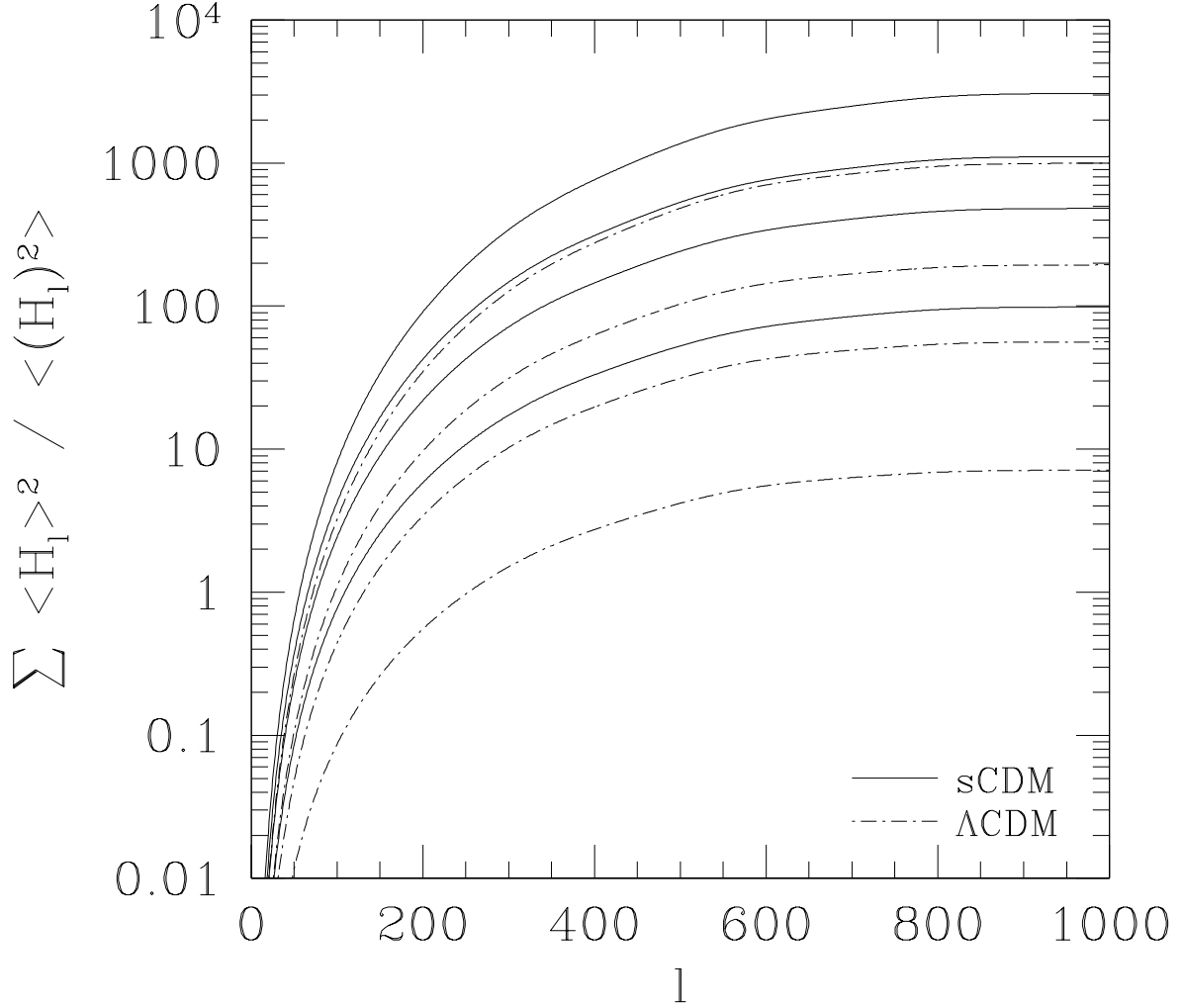


Fig. 3.— The cumulative signal-to-noise ratio. Solid and broken lines show the SCDM model and the Λ CDM model as in Fig. 1. For each model, the curves show the case in which $z = z_{\text{dec}}, 1, 0.5,$ and 0.2 .

REFERENCES

- Bardeen, J. M., Bond, J. R., Kaiser, N., and Szalay, A. S. 1986, *ApJ*, 304, 15
- Bouchet, F. R., Gispert, R., and Puget, J.-L. 1995, *Clustering in the Universe*, S. Maurogordato et al., Sigapore: Frontieres, 537
- Bunn, E. F., and White, M. 1997, *ApJ*, 480, 6
- Cayón, L., Martínez-González, E., and Sanz, J. L. 1993a, *ApJ*, 403, 471
- Cayón, L., Martínez-González, E., and Sanz, J. L. 1993b, *ApJ*, 413, 10
- Connolly, A. J., Csabai, I., Szalay, A. S., Koo, D. C., Kron, R. G., Munn, J. A. 1995, *AJ*, 110, 2655
- Gunn, J. E., and Weinberg, D. H. 1995, *Wide Field Spectroscopy and the Distant Universe*, S. J. Maddox and A. Aragón-Salamanca, Singapore: World Scientific, 3
- Kashlinsky, A. 1988, *ApJ*, 331, L1
- Knox, L. 1995, *Phys. Rev. D*, 52, 4307
- Linder, E. V. 1990a, *MNRAS*, 243, 353
- Linder, E. V. 1990b, *MNRAS*, 243, 362
- Linder, E. V. 1997, *A&A*, 323, 305
- Martínez-González, E., Sanz, J. L., and Cayón, L. 1997, *ApJ*, 484, 1
- Ostriker, J. P., and Steinhardt, P., J. 1995, *Nature*, 377, 600
- Readhead, A. C. S., Lawrence, C. R., Myers, S. T., Sargent, W. L. W., Hardebeck, H. E., and Moffet, A. T. 1989, *ApJ*, 346, 566
- Sasaki, M. 1989, *MNRAS*, 240, 415
- Seljak, U. 1994, *ApJ*, 436, 509
- Seljak, U. 1996, *ApJ*, 463, 1
- Seljak, U., and Zaldarriaga, M. 1996, *ApJ*, 469, 437
- Smoot, G. F. et al. 1992, *ApJ*, 396, L1
- Suginohara, M., Suginohara, T., and Spergel, D. N. 1997, in preparation
- Tomita, K. 1988, *PASJ*, 40, 751

Uson, J. M., and Wilkinson, D. T. 1984, *ApJ*, 283, 471

Watanabe, K., and Tomita, K. 1991, *ApJ*, 370, 481

Wright, E. L., Hinshaw, G., and Bennett, C. L. 1996, *ApJ*, 458, L53